

Short Communication

Cycling Stability of LiMnPO₄/C Composite Obtained by Different Processing Routes

Xiaopeng Lu^{1,3}, Xingning Wang^{1,3}, Min Wang², Haisheng Fang^{1,3,*}

¹ Key Laboratory of Advanced Battery Materials of Yunnan Province, Kunming University of Science and Technology, Kunming 650093, China

² Advanced Analysis and Measurement Center, Yunnan University, Kunming 650091, China

³ Faculty of Metallurgy and Energy Engineering, Kunming University of Science and Technology, Kunming 650093, China

*E-mail: hsfang1981@hotmail.com

Received: 15 November 2016 / Accepted: 19 February 2017 / Published: 12 March 2017

In this paper, LiMnPO₄ is composited with carbon black by two different processing routes and their cycling stability is compared. When the LiMnPO₄/C composite is finally processed by a ball milling treatment, amorphous domains are observed in LiMnPO₄, and the resulting composite shows an obvious impedance growth and capacity loss upon cycling. When the localized amorphization of LiMnPO₄ is eliminated by a post annealing treatment, the obtained composite shows an improved stability without any impedance growth upon cycling. Our result demonstrates that different processing route causes different crystallinity of LiMnPO₄ which has a big impact on the cycling stability of LiMnPO₄/C cathode.

Keywords: Lithium ion batteries; Cathode material; LiMnPO₄; Amorphization

1. INTRODUCTION

Olivine structured LiMPO₄ (M = Mn, Fe, Co, Ni) materials have attracted considerable attention as promising cathode materials for lithium ion batteries due to their low cost, low toxicity and good chemical stability [1-6]. Among these compositions, LiFePO₄ has already been commercialized, but its energy density is much lower than the more common LiCoO₂ cathode material due to the low potential of Fe³⁺/Fe²⁺ at 3.4 V vs. Li⁺/Li [1]. Therefore, another member LiMnPO₄ receives increased interest because of its ideal potential of Mn³⁺/Mn²⁺ at 4.1 V vs. Li⁺/Li [1]. Since the report of Li et al. [7], great efforts have been made to overcome the drawbacks of LiMnPO₄, and its performance especially the rate capability has been significantly improved by various methods [8-20] such as

carbon coating, particle size reduction and cation doping. However, only little attention was paid on the cycling stability of LiMnPO_4 in the previous reports [21-23], perhaps because olivine cathode materials are ordinarily thought to have good cycling stability. In fact, these reports [22,23] clearly demonstrated that the electrode of LiMnPO_4 would degrade upon cycling and a dense and protective carbon coating would be much beneficial. Herein we reveal a new factor which may highly affect the cycling stability of LiMnPO_4 . LiMnPO_4 is composited with carbon black by two different processing routes to prepare LiMnPO_4/C composite and their electrochemical performance is compared. We demonstrate that localized amorphization of LiMnPO_4 has a significant influence on the cycling stability of LiMnPO_4/C cathode.

2. EXPERIMENTAL

Chemicals of $\text{MnSO}_4 \cdot \text{H}_2\text{O}$, and H_3PO_4 with a molar ratio of 1:1 were dissolved in 40 mL distilled water at room temperature. The pH of the solution was adjusted to around 10 by addition of LiOH solution under vigorous stirring. The obtained suspension was transferred into a Teflon-lined stainless steel autoclave and heated in an oven at 200 °C for 10 h. The precipitated LiMnPO_4 was fully washed with distilled water, filtrated, and dried at 120 °C. To prepare LiMnPO_4/C composite, the as-prepared LiMnPO_4 was composited with carbon black via two different routes: (1) the as-prepared LiMnPO_4 was firstly mixed with 20 wt. % of carbon black, and then annealed at 700 °C for 2 h in N_2 , and finally ball-milled for 4 h. The obtained composite was denoted as LiMnPO_4/C -1; (2) the as-prepared LiMnPO_4 was ball-milled with 20 wt. % of carbon black for 4 h and then annealed at 700 °C for 2 h in N_2 . The obtained composite was denoted as LiMnPO_4/C -2.

Powder X-ray diffraction (XRD) patterns of samples were recorded on apparatus (DMAX2500, Rigaku, Japan) using CuK_α radiation. The particle size, morphology and microstructure of samples were observed by scanning electron microscope (SEM, JEOL, JSM-5600LV) and transmission electron microscope (TEM, TecnaiG2 F20, FEI).

Electrochemical characterization of samples was performed using CR2025 coin-type cell. For cathode fabrication, LiMnPO_4/C composite, carbon black and polyvinylidene fluoride with a weight ratio of 9:1:1 were mixed in *N*-methyl pyrrolidinone. The slurry thus obtained was pasted onto Al foil and dried at 100 °C for 10 h in vacuum. All cells consisted of cathode and lithium foil anode which were separated by a porous polypropylene film and electrolyte of 1 M LiPF_6 in EC:EMC:DMC (1:1:1 in volume), and were assembled in a dry Ar-filled glove box. The cells were charged and discharged between 2.5 and 4.7 V at a constant current density of 30 mA g^{-1} (equal to 0.2 C). Electrochemical impedance spectroscopy (EIS) was performed on a CHI660A Electrochemical Workstation in a frequency range from 0.1 to 100 kHz with an AC signal of 5 mV.

3. RESULTS AND DISCUSSION

Fig. 1 shows XRD patterns of the two LiMnPO_4/C composites. Both samples can be identified as a single orthorhombic phase of LiMnPO_4 , and no peaks of carbon can be observed in both patterns,

indicating that the carbon exists as an amorphous form in the composite. Meanwhile, there also exists some difference between the two patterns. It is obvious that the diffraction peaks of $\text{LiMnPO}_4/\text{C-1}$ (Fig. 1a) are weaker and broader than those of $\text{LiMnPO}_4/\text{C-2}$ (Fig. 1b). Variation in intensity and width of diffraction peaks may be associated with the difference in crystal size and/or crystallinity of the two samples.

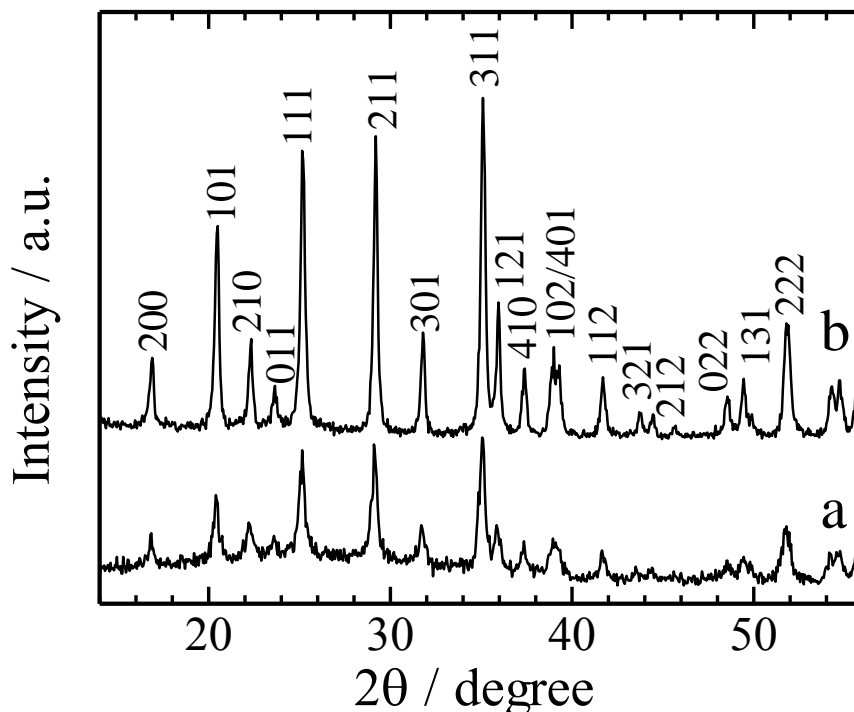


Figure 1. XRD patterns of the two LiMnPO_4/C composites: (a) $\text{LiMnPO}_4/\text{C-1}$, (b) $\text{LiMnPO}_4/\text{C-2}$.

Fig. 2 shows SEM and TEM images of the two LiMnPO_4/C composites. The morphology and particle size of the two composites are quite similar as shown in Fig. 2a and b, which may exclude size effect as a main cause for the observed variation in the two XRD patterns. TEM measurement reveals that the variation of XRD diffraction peaks should be originated from the different crystallinity of LiMnPO_4 in the two composites. It is well-known that ball milling treatment not only may cause particle size reduction, but also may give rise to amorphization of the milled material. Meanwhile, it is also known that the amorphization induced by ball milling can be eliminated by a simple post annealing treatment. This is the case in the present work as indicated by TEM in Fig. 2c and d. For the $\text{LiMnPO}_4/\text{C-1}$ sample which was finally processed by a ball milling treatment, amorphous domains can be easily found in the LiMnPO_4 crystal as represented in Fig. 2c, while for the $\text{LiMnPO}_4/\text{C-2}$ sample which was finally processed by a post annealing treatment, amorphization induced by ball milling has been eliminated and fine crystal fringes of LiMnPO_4 crystal are clearly observed in Fig. 2d. Hence, the two LiMnPO_4/C composites show some difference in crystallinity of LiMnPO_4 : the $\text{LiMnPO}_4/\text{C-1}$ sample presents localized amorphous domains in LiMnPO_4 , while the $\text{LiMnPO}_4/\text{C-2}$ sample possesses highly crystallized LiMnPO_4 .

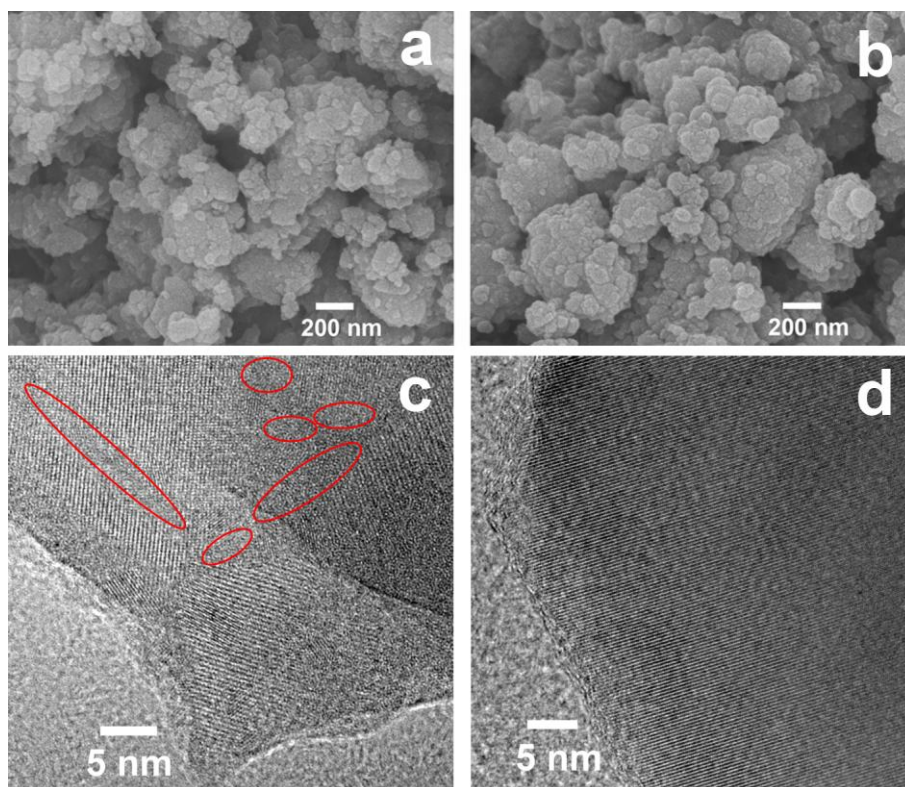


Figure 2. SEM and TEM images of the two LiMnPO_4/C composites: (a and c) $\text{LiMnPO}_4/\text{C-1}$, (b and d) $\text{LiMnPO}_4/\text{C-2}$.

To investigate the electrochemical performance of the two LiMnPO_4/C composites, charge and discharge test at a constant current density of 30 mA g^{-1} has been performed, and representative curves as well as cycling performance are shown in Fig. 3. On the one hand, the two samples show a similar electrochemical activity and only a reversible capacity up to $\sim 85 \text{ mAh g}^{-1}$ can be delivered. Table 1 compares the reversible capacity of our sample with other LiMnPO_4/C reported in available literature [8,12,24-27]. It is seen that the capacity of LiMnPO_4/C is not only dependent on synthesis method, but also on synthesis parameters and carbon content. It is highly expected that the electrochemical activity of our hydrothermally synthesized LiMnPO_4 can be effectively enhanced by tailoring synthesis parameters such as solution pH value and carbon content. In addition, cation doping is another way to improve the property of LiMnPO_4 which has been demonstrated in our previous report [28,29]. Work is in progress in both directions.

On the other hand, it is seen that the two composites have distinct electrode stability upon cycling. As shown in Fig. 3a and c, the $\text{LiMnPO}_4/\text{C-1}$ sample suffers an apparent fade in capacity upon cycling. After 172 cycles, the capacity decreases from a maximum of 80.9 mAh g^{-1} to 48.5 mAh g^{-1} . Moreover, growing polarization is observed between charge and discharge curves in the extended cycles. This behavior indicates an increased internal impedance upon cycling. Indeed an obvious impedance growth is observed after 172 cycles as compared to that after 20 cycles for the $\text{LiMnPO}_4/\text{C-1}$ sample as shown in Fig. 4. By contrast, different electrochemical behavior is observed for the $\text{LiMnPO}_4/\text{C-2}$ sample. As shown in Fig. 3b and d, a gradual increase in capacity during the first

several ten cycles is observed and then a stable capacity maintains in the subsequent cycles. Meanwhile, polarization growth between charge and discharge curves does not appear upon cycling. After 172 cycles, the LiMnPO₄/C-2 sample can still deliver a capacity of 85 mAh g⁻¹, and the voltage plateaus are still well maintained. Correspondingly, impedance growth is not involved upon cycling for the LiMnPO₄/C-2 sample as shown in Fig. 4. These observations clearly show that cycling instability of LiMnPO₄/C is accompanied by impedance growth of the electrode. Similar phenomenon has long been observed on LiCoO₂ cathode. Aurbach et al. and Dahn et al.[30,31] reported that capacity loss of LiCoO₂ was associated with impedance growth which was caused by some side reactions involving on the surface of electrode upon cycling. In our work, the localized amorphous domains in LiMnPO₄ is less stable and undesirable side reactions may more easily arise on these microarea with electrolyte, which in turn leads to impedance growth, polarization increase and capacity loss for the LiMnPO₄/C upon cycling. In the paper reported by J. Moskon et al. [23], they observed pronounced gradual amorphization of the olivine crystallites in degradation process of LiMnPO₄ electrode upon cycling. Their observation suggests that the degradation of LiMnPO₄ electrode can cause amorphization of the olivine crystallites. Clearly, our observation is well consistent with what is observed in their work [23]. From the above results, we may conclude that the localized amorphous domains in LiMnPO₄ has a detrimental effect on the cycling stability of LiMnPO₄/C composite. This finding will have important implication for rational synthesis and processing of LiMnPO₄ to optimize its performance.

Table 1. Comparison of reversible capacity of our LiMnPO₄/C sample with other LiMnPO₄/C samples reported in available literature

synthesis method	carbon content	capacity (mAh g ⁻¹)	literature
hydrothermal reaction	20 wt. %	~85, 0.2 C	this work
direct precipitation	16.7 wt %	~80, 0.05C	ref. 8
precursor-based synthesis	50 wt %	~60, 0.2 C	ref. 24
polyol method	20 wt. %	~141, 0.1C	ref. 12
ultrasonic spray	10 wt. %	~100, 0.2C	ref. 25
pyrolysis	20 wt. %	~120, 0.2C	
solvothermal synthesis (water/PEG)	4 wt%	~55, 0.2C (pH: 4.99) ~105, 0.2C (pH: 6.46)	ref. 26
solvothermal synthesis (water/DEG)	9 wt%	~130, 0.2C(150 °C-6h) ~130, 0.2C(190 °C-3h)	ref. 27

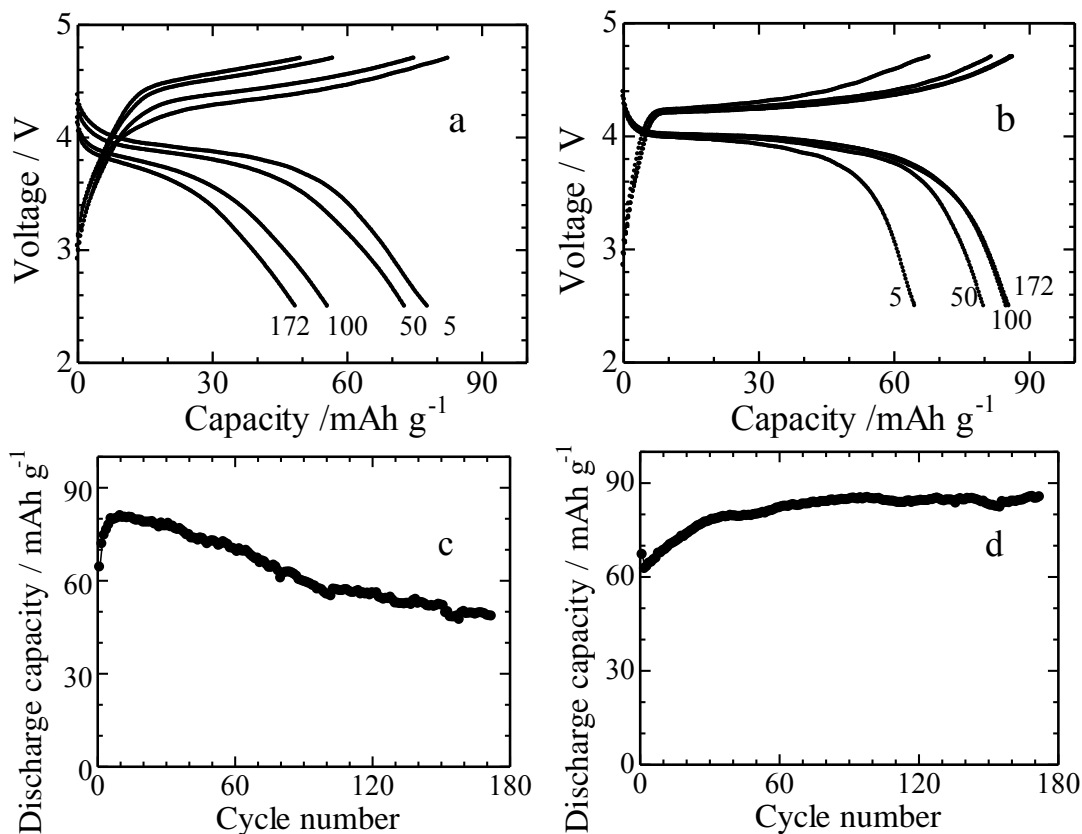


Figure 3. Representative charge-discharge curves and cycling performance of the two LiMnPO₄/C composites: (a and c) LiMnPO₄/C-1, (b and d) LiMnPO₄/C-2. Cells were charged and discharged at a constant current density of 30 mA g⁻¹ in a voltage range of 2.5 to 4.7 V.

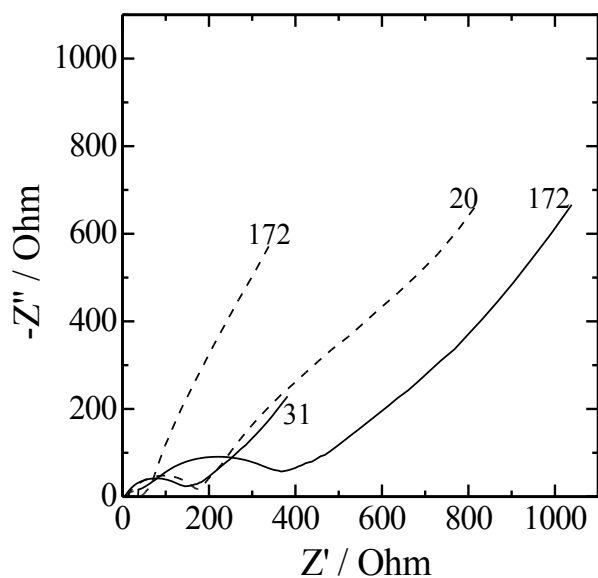


Figure 4. Impedance spectra of the two LiMnPO₄/C composites measured at the fully discharged state. Solid line: LiMnPO₄/C-1, and dashed line: LiMnPO₄/C-2. Before impedance measurement, cells were charged and discharged at a constant current density of 30 mA g⁻¹ in a voltage range of 2.5 to 4.7 V.

4. CONCLUSIONS

Two LiMnPO₄/C composites were obtained via two different processing routes, and different impedance evolution and electrode stability upon cycling were observed due to the different crystallinity of LiMnPO₄ in the two composites. Our result demonstrates that the localized amorphization of LiMnPO₄ may cause impedance growth, polarization increase and capacity degradation of the LiMnPO₄/C cathode upon cycling.

ACKNOWLEDGEMENTS

This work is supported by the National Natural Science Foundation of China [Grant numbers 51664031 and 51304098].

References

1. A. K. Padhi, K. S. Nanjundaswamy, and J. B. Goodenough, *J. Electrochem. Soc.*, 144 (1997) 1188.
2. C. Delacourt, P. Poizot, S. Levasseur, and C. Masquelier, *Electrochem. Solid-State Lett.*, 9 (2006) A352.
3. S. Y. Chung, J. T. Bloking, and Y.M. Chiang, *Nat. Mater.*, 1 (2002) 123.
4. N. Ravet, Y. Chouinard, J. F. Magnan, S. Besner, M. Gauthier, and M. Armand, *J. Power Sources*, 97-98 (2001) 503.
5. H. Huang, S. C. Yin, and L. F. Nazar, *Electrochem. Solid-State Lett.*, 4 (2001) A170.
6. B. Kang and G. Ceder, *Nature*, 458 (2009) 190.
7. G. Li, H. Azuma, and M. Tohda, *Electrochem. Solid-State Lett.*, 5 (2002) 135.
8. C. Delacourt, P. Poizot, M. Morcrette, J. M. Tarascon, and C. Masquelier, *Chem. Mater.*, 16 (2004) 93.
9. N. H. Kwon, T. Drezen, I. Exnar, I. Teerlinck, M. Isono, and M. Graetzel, *Electrochem. Solid-State Lett.*, 9 (2006) A277.
10. G. Y. Chen, J. D. Wilcox, and T. J. Richardson, *Electrochem. Solid-State Lett.*, 11 (2008) A190.
11. T. Shiratsuchi, S. Okada, T. Doi, and J. Yamaki, *Electrochim. Acta*, 54 (2009) 3145.
12. D. Y. Wang, H. Buqa, M. Crouzet, G. Deghenghi, T. Drezen, I. Exnar, N. H. Kwon, J. H. Miners, L. Poletto, and M. Graetzel, *J. Power Sources*, 189 (2009) 624.
13. S. K. Martha, J. Grinblat, O. Haik, E. Zinigrad, T. Drezen, and D. Aurbach, *Angew. Chem. Int. Ed.*, 48 (2009) 8559.
14. D. Choi, D. Wang, I. T. Bae, J. Xiao, Z. Nie, W. Wang, V. V. Viswanathan, Y. J. Lee, J. G. Zhang, G. L. Graff, Z. Yang, and J. Liu, *Nano Lett.*, 10 (2010) 2799.
15. J. Kim, D. H. Seo, S. W. Kim, Y. U. Park, and K. Kang, *Chem. Commun.*, 46 (2010) 1305.
16. H. Wang, Y. Yang, Y. Liang, L. F. Cui, H. Sanchez Casalongue, Y. Li, G. Hong, Y. Cui, and H. Dai, *Angew. Chem. Int. Ed.*, 50 (2011) 7364.
17. H. Yoo, M. Jo, B. Jin, H. Kim, and J. Cho, *Adv. Energy Mater.*, 1 (2011) 347.
18. L. Wu, S. K. Zhong, F. Lv, and J. Q. Liu, *Mater. Lett.*, 110 (2013) 38.
19. S. Liu, H. S. Fang, E. R. Dai, B. Yang, Y. C. Yao, W. H. Ma, and Y. N. Dai, *Electrochim. Acta*, 116 (2014) 97.
20. A. Gutierrez, R. Qiao, L. Wang, W. Yang, F. Wang, and A. Manthiram, *Chem. Mater.*, 26 (2014) 3018.
21. S. K. Martha, B. Markovsky, J. Grinblat, Y. Gofer, O. Haik, E. Zinigrad, D. Aurbach, T. Drezen, D. Y. Wang, G. Deghenghi, and I. Exnar, *J. Electrochem. Soc.*, 156 (2009) A541.
22. N. S. Norberg and R. Kostecky, *J. Electrochem. Soc.*, 159 (2012) A1431.

23. J. Moskon, M. Pivko, I. Jerman, E. Tchernychov, N. Zabukovec Logar, M. Zorko, V. S. Selih, R. Dominko, and M. Gaberscek, *J. Power Sources*, 303 (2016) 97.
24. N. N. Bramnik and H. Ehrenberg, *J. Alloys Compd.*, 464 (2008) 259.
25. S. M. Oh, S. W. Oh, C. S. Yoon, B. Scrosati, K. Amine and Y. K. Sun, *Adv. Funct. Mater.*, 20 (2010) 3260.
26. S. L. Yang, R. G. Ma, M. J. Hu, L. J. Xi, Z. G. Lu and C. Y. Chung, *J. Mater. Chem.*, 22(2012) 25402.
27. K. Zhu 1, W. Zhang 1, J. Du, X. Liu, J. Tian, H. Ma, S. Liu and Z. Shan, *J. Power Sources*, 300 (2015) 139.
28. C. L. Hu, H. H. Yi, H. S. Fang, B. Yang, Y. C. Yao, W. H. Ma and Y. N. Dai, *Electrochem. Commun.*, 12 (2010) 1784.
29. H. S. Fang, E. R. Dai, K. Yang, B. Yang, Y. C. Yao, W. H. Ma, and Y. N. Dai, *Int. J. Electrochem. Sci.*, 7 (2012) 11827.
30. D. Aurbach, B. Markovsky, A. Rodkin, E. Levi, Y. S. Cohen, H. J. Kim, and M. Schmidt, *Electrochim. Acta*, 47 (2002) 4291.
31. Z. H. Chen and J. R. Dahn, *Electrochim. Acta*, 49 (2004) 1079.

© 2017 The Authors. Published by ESG (www.electrochemsci.org). This article is an open access article distributed under the terms and conditions of the Creative Commons Attribution license (<http://creativecommons.org/licenses/by/4.0/>).